Modelling the effect of extreme sea surface temperature events on the demography of an age-structured albatross population

Deborah Pardo[1,2]*, Stéphanie Jenouvrier[1,3]*, Henri Weimerskirch[1] and Christophe Barbraud[1]

[1]Centre d'Etudes Biologiques de Chizé, UMR7372 CNRS, F-79360 Villiers-en-Bois, France

[2]British Antarctic Survey, Madingley Road High cross, Cambridge CB30ET, UK

[3]Woods Hole Oceanographic Institution, Mailstop 50, Woods Hole, MA 02543, USA

* Equal contributions

Correspondence to Deborah Pardo, deborah.pardo@gmail.com, 00447450869469

Climate changes include concurrent variations in environmental mean, variance and extremes and it is challenging to understand their respective impact on wild populations, especially when contrasted age-dependent responses to climate occur. We assessed how changes in mean and standard deviation of Sea Surface Temperature (SST), frequency and magnitude of warm SST Extreme Climatic Events (ECE) influenced the stochastic population growth rate $\log(\lambda_s)$ and age structure of a black-browed albatross population.

For changes in SST around historical levels observed since 1982, changes in standard deviation had a larger (threefold) and negative impact on $\log(\lambda_s)$ compared to changes in mean. The historical SST mean was lower than an optimal SST value when $\log(\lambda_s)$ was maximised. Thus larger environmental mean increased the occurrence of SST close to this optimum that buffered the negative effect of ECE mediated through increases in frequency and magnitude. This 'climate safety margin' (i.e. difference between optimal and historical climatic conditions) and the specific shape of the population growth rate response to climate for a species determine how ECE affect the population. Furthermore, increases in either mean or standard deviation of the SST distribution led to a younger population, with potentially important conservation implications for black-browed albatrosses.

Keywords: age, climate change, IPCC, matrix population model, sensitivity analysis, survival

1. Introduction

The Intergovernmental Panel on Climate Change (IPCC) research group outlined that special attention should be put forth on the impact of Extreme Climatic Events (ECE) on human societies and ecosystems [1]. Marked temperature anomalies and associated heat waves may become more of a common environmental feature by the end of the century that our society and wild populations will have to adjust to, in conjunction with an adjustment to overall global warming [2]. Yet, assessing changes in ECE remains challenging given their rarity by definition [3] and the difficulty to model and understand their ecological effects at different spatio-temporal scales and biological levels [4–6]. Extreme events can be defined in many ways; throughout this paper, a climatological definition will be used as the occurrence of a value as rare as or rarer than the 5^{th} and 95^{th} percentile of the distribution of observed values in a climatic variable of interest (e.g. temperature, precipitation) over a specific historical time period [7].

The effects of climate change on wild populations have been extensively studied but most studies focused on the effect of changes in mean temperature and/or precipitation regimes on phenology, physiology, behaviour and demography [8–10]. In recent years the number of studies investigating the effects of ECE in wild populations has been increasing [11–13]. There is now empirical evidence that ECE can have strong ecological effects as they can lead to local extinctions [14], changes in sex-ratio [15], disease proliferation [16] and even reset community composition [17].

However, understanding the respective biological responses to the effects of changes in mean climate and climate variability – especially ECE – requires more research [7,18–22]. Projections of population responses based on mean temperature changes alone can differ substantially from those incorporating changes to the variability, including extreme events [23,24]. Furthermore, different life-history stages, phenotypes or age-classes can respond

differently to the same climatic variable [25–27]. For example, Jenouvrier *et al.* [28] showed that extreme sea ice years affected foraging behaviour, body condition, vital rates and population growth rate of the southern fulmar (*Fulmarus glacialoides*), and individuals of higher quality were less impacted by these extreme events. Therefore, changes in ECE can strongly alter not only the population growth rate but also the structure of populations. For example, during the 2003 heat wave in Europe, more than 70 000 human deaths were recorded, with the most vulnerable persons being young and older individuals [29], which affected the age pyramid.

Here, we focus on the long-lived black-browed albatross (*Thalassarche melanophris*) using a 50 years longitudinal dataset including several thousands of individuals. Previous studies have shown that survival and fecundity of black-browed albatrosses breeding in Kerguelen, French Sub-Antarctic territories, varied in response to changes in Sea Surface Temperature (SST) in their foraging zones during the breeding season [30–32]. Pardo *et al*. [33] showed that fecundity and survival responses to changes in SST were different between age-classes, with larger effects on young and old breeders than on middle-aged birds. To understand the respective impacts of increasing mean and variability of SST, as well as frequency and magnitude of extreme SST events on population growth and structure, we constructed an age-structured stochastic matrix population model in which young, middle-aged and old breeders responded differently to changes in SST. We had 3 specific aims (Fig. 1 bottom):

1) Determine the influence of changes in the mean and standard deviation of the historical SST distribution on the characteristics of warm ECE (frequency and magnitude);

2) Determine the influence of changes in the mean and standard deviation of the historical SST distribution on the stochastic population growth rate and stable age distribution;
3) Study the effects of ECE on stochastic population growth rate and stable age distribution.

We address these questions at two different ranges of SST that contrast the historical versus future climate change: i) at the local scale around the historical SST distribution by using a sensitivity analysis based on the partial derivative method, and ii) an analysis over a wider range of climatic parameters with various scenarios of change in the mean or standard deviation of the SST distribution using scatter plots.

2. Material and methods

(a) Species life cycle

Black-browed albatross are large Procellariforms (3 - 4 kg, 2 - 2.5 m wingspan) that breed on Sub-Antarctic islands during the austral summer. Birds arrive in September and lay a single egg in October that will hatch in December. Both parents alternate care at the nest during incubation of the egg and brooding of the young chick, then provision the large chick that fledges in late March at a size similar to that of an adult. This study focuses on black-browed albatross breeding at Canyon des Sourcils Noirs (49.4°S – 70.1°E), Kerguelen Islands. Each year since 1978, pair members were identified with a stainless steel band. In addition, all fledglings, unringed breeding individuals and non-breeding individuals attending the colony were marked. The average age at first breeding is 9.7 and can range from 5 to 15 years old [34]. During breeding, black-browed albatrosses forage in northeast and southeast regions of the peri-insular Kerguelen shelf [30–32]. Their diet at that period is composed by fish (73%), penguin carrion (14%) and squids (10%) [35]. They are known to strongly

interact with long-line and trawl fisheries targeting patagonian toothfish (*Dissostichus eleginoides*) and mackerel icefish (*Champsocephalus gunnari)* to feed on discards and baits [36]. Such interactions can affect black-browed albatross demography and dynamics [37]. In winter, breeding adults migrate to southeast Australia and north of Tasmania in less than a week, where they remain until the next breeding season and occasionally follow longliners fishing for southern bluefin tuna (*Thunnus thynnus*) and other tuna species in their wintering zone [38].

(b) Sea surface temperature

Historical SST were extracted from satellite data from 1982 to 2015 in a spatial sector where most birds from this colony forage during the breeding season (from October to March; International Research Institute for climate and Society http://iridl.ldeo.columbia.edu/; see map in Pardo *et al*. [33]). SST is thought to be a proxy of food availability in the marine environment and has been found in several studies to have an influence on breeding parameters as well as survival rates in this population [30,32,39].

Seasonal means in historical SST data over 34 years were used to determine thresholds of ECE, so that values below the 5^{th} percentile (3.52°C) were considered as cold SST ECE and above the 95^{th} percentile (4.63°C) as warm SST ECE (Fig. 1, top left panel). As IPCC predicts an increase in Earth surface temperature (including SST) and an increase in the frequency and magnitude of heat waves in particular, we focussed mainly on the influence of the warmer temperatures in this manuscript [1]. The historical SST followed a normal distribution (Anderson-Darling test: $p=0.13$) with two parameters: the mean ($\mu= 3.95$°C at baseline conditions based on the historical data) and the standard deviation ($\sigma= 0.35$ at baseline conditions; Fig. 1 bottom left panel). We derived various scenarios based on the normal distribution fitted on historical SST data: the baseline scenario, a scenario when mean

temperature increases up to μ + 1°C, and a scenario when standard deviation increases up to σ * 2. These scenarios resulted in demographic rates that were in a realistic range of variations (electronic supplementary material A). Two characteristics of warm ECE were calculated from a SST vector obtained by sampling into the fitted distributions (SST vector length of 10,000): the frequency and magnitude of warm ECE. The frequency of warm ECE was calculated as the number of extreme years divided by the total number of years multiplied by 100 (baseline frequency of warm ECE = 2.86%), and the magnitude of warm ECE was the warmest temperature (i.e. maximum value of the SST vector, baseline magnitude of warm ECE = 5.28°C).

(c) Population model

To calculate the population growth rate and structure, we constructed an age-structured matrix model using a pre-breeding census [40] based on a life cycle of 34 age-classes where individuals older than 34 years old remain in the last stage (Fig. 1 bottom right panel). We projected the population between time t and t+1 using the following equation: $\mathbf{n}_{(t+1)} = \mathbf{A}_t \, \mathbf{n}_{(t)}$ where $\mathbf{n}_{(t)}$ is the population vector at time t including the 34 age-classes and $\mathbf{A}_t$ is the projection matrix containing the age-specific vital rates [40]. Thus, the projection matrix $\mathbf{A}_t$ depended on SST in each year, with vital rates projected from the specific functional relationships with from Pardo *et al*. [33] (Fig. 1 top right panel).

Vital rates were projected using linear and quadratic functional relationships with SST on the logit scale for four different vital rates (Fig. 1 top right panel): apparent survival probability, return probability to the breeding grounds, breeding probability (laying an egg) given return and breeding success probability (chick fledged) given breeding. Survival, return, breeding and success probabilities were estimated for all individuals according to their age. Vital rates and SST varied between the following age-classes: young from 5 to 10 years old,

middle-aged from 11 to 26 years old for return, breeding and success probabilities and from 11 to 29 for survival probability [33]. After age 26 for success probability or 29 for survival probability, birds were in the old age-class until the maximum age observed (i.e., 34 years old). There was no old age-class for return and breeding probabilities (electronic supplementary material B). Breeding experience was not included in this study.

Fecundity was defined as the product of age-dependent return, breeding and success probabilities multiplied by the sex ratio at birth (assumed even [37]) and juvenile survival. We used an estimate of juvenile survival probability from Nevoux *et al.* [41] assuming that juvenile survival (Sj) was constant over the first 5 years ($Sj_{0\text{-}5} = Sj_{0\text{-}1}*Sj_{1\text{-}2}*Sj_{2\text{-}3}*Sj_{3\text{-}4}*Sj_{4\text{-}5} =$ 0.281). There was no data to estimate annual variation of juvenile survival before recruitment because young birds stay at sea permanently from fledging until first return on land. Thus, annual juvenile survival was set to constant ($Sj = 0.776$ [fifth root of 0.281 for $Sj_{0\text{-}5}$]). Apparent survival can be an underestimation of true survival due to permanent emigration but in highly philopatric species such as albatrosses, we do not expect it to be large (< 2%; [42]). Rolland et al. [37] estimated the annual immigration rate at 0.044 and as we had no information on how it might be linked with SST or age, we focussed on local population dynamics.

A SST value was drawn randomly 10 000 times from the normal distribution fitted on historical SST data and altered to simulate more ECE. The stochastic population growth rate $\log(\lambda_s)$ and the stable age distribution (asymptotic relative proportion of individuals in each age-class) were then calculated following the approach described in Chap. 14.1 of Caswell [39] using numerical simulation. All analyses were performed in program MATLAB [43].

(d) Local sensitivity analysis

We first performed a local sensitivity analysis by calculating numerically the partial derivative of frequency and magnitude of warm ECE events (climatic output y) over 10 000 time steps with respect to the mean and standard deviation of the normal distribution fitted on historical SST data (Aim 1, Fig. 1 bottom panel). In addition, we performed a local sensitivity analysis of the growth rate and stable age distribution (demographic output y) with respect to SST parameters following the same approach (Aim 2, Fig. 1 bottom panel).

We evaluated the sensitivity of a climatic or demographic output of the model (y) with respect to the mean or standard deviation of the SST distribution (input x) by calculating numerically the partial derivative dx/dy. We perturbed the input by a small perturbation such as the perturbed input is $x_p = x(1 \pm 0.001)$. We performed 100 simulations for each positive and negative perturbation, and estimated as $dx/dy = (y-y_p)/(x-x_p)$ for each simulation and perturbation. The sensitivity is measured as the average of dx/dy over 200 simulations.

(e) Effect of SST on stochastic population growth rate

Since the results of the sensitivity analysis based on the partial derivative were very local, we performed an analysis over a wider range of the SST distribution parameters similar to a global sensitivity analysis. Our aim was to illustrate the contrasted effects of changes in SST distribution parameters between the historical and future projected ranges of SST. Thus, we chose a simple but useful approach computing the scatter plots of the stochastic population growth rate against SST distribution parameters as well as the frequency and magnitude of ECE (Aim 3, Fig. 1 bottom panel). Starting from the baseline parameters of the SST distribution, we varied the mean by up to 1°C [1] and the standard deviation up to twice the baseline value ($\sigma = 0.70$). Changes in the mean and standard deviation of the distribution were varied independently.

3. Results

(a) Sensitivity of climatic output (Aim 1)

The local sensitivity analysis of climatic output showed the relative effects of a unit of change in the two parameters of the historical SST distribution (μ, σ) on the frequency and magnitude of warm ECE (Fig. 2). Increasing the mean or standard deviation increased the frequency and magnitude of warm ECE. A unit of change in standard deviation (σ) had a larger effect on both frequency (1.6 times larger) and magnitude of warm ECE (3 times larger) than a unit of change in the mean (μ).

(b) Sensitivity of demographic output (Aim 2)

The sensitivity of $\log(\lambda_s)$ with respect to the standard deviation was negative while the sensitivity of $\log(\lambda_s)$ with respect to the mean was positive (Fig. 3). A unit of change in standard deviation (σ) had a larger effect on $\log(\lambda_s)$ (~3 times larger) than a unit of change in the mean (μ) (Fig. 3).

Considering the stable age distribution, in the baseline conditions 44% of the population was 5 years old or less (Fig. 4 top). The sensitivity analysis revealed that changes in mean or standard deviation of the SST distribution affected the proportion of individuals in all age-classes (Fig. 4 bottom). A unit change in mean had a larger influence than a unit change in the standard deviation, and their relative effects had opposite sign in middle-aged classes. However, the sensitivities of the stable age distribution with respect to a unit change in mean and/or standard deviation were both positive for age-classes from 2 to 5 years old and both negative for old age-classes from 28 to 34+ years old (Fig. 4 bottom). To summarise, the number of individuals in the immature age-classes (under 5 years old) increased and the number of individuals in the oldest age-classes decreased when mean or standard deviation of the SST distribution increased, resulting in a younger population.

(c) Relationship between ECE, population growth and SST distribution parameters (Aim 3)

In the baseline conditions, the stochastic growth rate was $\log(\lambda_s) = -0.033$ meaning that the local population of black-browed albatross is currently decreasing annually by 3.3%.

As the previous sensitivity analysis was very local, we also investigated the relationships, relative to baseline levels, between $\log(\lambda_s)$ and the climatic ECE characteristics on a wider range of change in SST distribution parameters (Fig. 5). First, figure 5 shows that $\log(\lambda_s)$ was maximized at slightly warmer values of mean SST than present (i.e. observed mean + 0.1°C), with an optimal value of $\log(\lambda_s)$ of -0.032. $\log(\lambda_s)$ declined as mean SST became warmer or colder. Interestingly, the effect of colder SST was stronger than the effect of warmer SST (Fig. 5). There was a large plateau around the optimal $\log(\lambda_s)$ value (-0.2°C to +0.4°C). Over the range of mean SST values shown here, the effect of standard deviation was negative, lowering $\log(\lambda_s)$ by up to 0.02.

Second, figure 6 shows: i) how changes to baseline SST distribution parameters (shown with increased marker size on the mean and standard deviation) lead to increased climatic ECE characteristics (frequency and magnitude on the x-axis), and ii) how changes in the frequency and magnitude of ECE lead to changes in $\log(\lambda_s)$ (y-axis). Mean and standard deviation parameters both influenced the frequency and magnitude of warm ECE. Mean SST had by far the strongest impact on the frequency of ECE (Fig. 6 top) after a small plateau around historical level up to 8% ECE frequency. For an increase of 1°C, $\log(\lambda_s)$ declined to -0.064 when 80% of SST were considered extreme according to the historical climatological definition. Changes in the standard deviation affected the frequency of warm ECE to a much lesser extent for the range explored here (up to 20% extreme event frequency for a doubled value of standard deviation) and the minimum $\log(\lambda_s)$ reached -0.053 (Fig. 6 top). Opposite

patterns occurred with the magnitude of warm ECE (Fig. 6 bottom). A steeper decline in $\log(\lambda_s)$ resulted when changes in the magnitude were caused by a change in the standard deviation of the SST distribution rather than a change in the mean.

To summarize, for changes in SST around the historical levels observed since 1982, the standard deviation of the SST distribution had a larger and negative impact on $\log(\lambda_s)$ compared to a change in the mean.

4. Discussion

Using a black-browed albatross demographic model incorporating age and SST-dependent vital rates, we have characterized the impact of changes in the mean and standard deviation of the climatic distribution on the frequency and magnitude of ECE as well as on the population growth and structure. We highlighted opposite as well as parallel effects of changes in mean and standard deviation on the growth rate and age-structure of the population. In addition, we showed how the impact of ECE frequency and magnitude on population growth rate is mediated through change in mean or standard deviation of the SST distribution. Below, we discuss some methodological aspects of our approach and how future studies could build on our framework toward a more comprehensive understanding of the impact of ECE on population growth and structure.

(a) Effect of changes in the parameters of the SST distribution on the stochastic population growth rate

Several recent theoretical studies have emphasized that the relative effects of environmental standard deviation and mean on stochastic population growth rate $\log(\lambda_s)$ are expected from the curvature of the population growth response to the environment (referred as the population response function): a concave response results in a negative effect of

environmental standard deviation on $\log(\lambda_s)$ while the opposite occurs for a convex response (see review in Lawson *et al.* [21]). Figure 5 depicts such a population response function for the black-browed albatross, and shows that the response is concave around historical levels. As expected, the effect of SST standard deviation was negative on black-browed albatross $\log(\lambda_s)$.

We demonstrated that, around the historical values of SST, a change in the standard deviation of the SST distribution had a larger effect on the black-browed albatross $\log(\lambda_s)$ than a change in SST mean. García-Carreras & Reuman [44] concluded that many populations close to their optimal environment are likely to be more sensitive to a change in the variability of the environment rather than the mean. In contrast, changes in mean conditions are likely to have a greater impact than changes in variability on populations far from their optimal environment. Our results at both the historical (Fig. 3) and for a wider range of SST distribution parameters (Fig. 5) are in agreement with these theoretical expectations because: (i) we observed a peaked response function of the black-browed albatross $\log(\lambda_s)$ to SST, and (ii) the historical variation of SST are close the optimal value for the black-browed albatross.

Noteworthy, the sensitivity of the black-browed albatross $\log(\lambda_s)$ with respect to the SST standard deviation was negative while its sensitivity with respect to the SST mean was positive. This pattern is expected [44] because the $\log(\lambda_s)$ is maximized at warmer values of mean SST than present (i.e. $SST_{OPT} = SST_{HISTORICAL} + 0.1°C$). As a result, larger environmental standard deviation would cause more SST values far from the optimum, while larger mean would cause more SST values close to the optimum. This pattern echoes results from empirical studies on ectotherms [45,46]: a positive shift in mean temperature (T) will decrease mean fitness in tropical ectothermic species, but will increase fitness at higher latitudes because tropical species are experiencing mean annual temperatures ($T_{HISTORICAL}$)

very close to their optimal temperatures (T_{OPT}), while the opposite occurs at higher latitudes [45]. Specifically, ectothermic species 'thermal safety margins' ($T_{OPT} - T_{HISTORICAL}$) is typically 1 – 4°C in the tropics and increase markedly with latitude, up to 10°C or more at higher latitudes.

(b) Effect of ECE on the stochastic population growth rate

The frequency and magnitude of warm ECE depended on the two parameters of the normal SST historical distribution. Thus, it is not straightforward to understand the respective effect of ECE through their response to a change in the environmental mean and standard deviation. Around the historical value, our sensitivity analysis of the climate outputs showed that both the frequency and magnitude of ECE were more influenced by a change in the standard deviation rather than the mean of the SST distribution (Fig. 2). However, over a wider range of parameters (Fig. 6), the SST mean had a stronger impact on the frequency of warm ECE, especially beyond SST_{OPT}, and the standard deviation parameter influenced greatly the magnitude of ECE.

The effect of warm ECE, was negative on the black-browed albatross $\log(\lambda_s)$ (Fig. 5). In addition, higher frequency and magnitude of ECE mostly decreased $\log(\lambda_s)$, although it depended on the path through which such changes occurred - i.e. changes in the mean, or standard deviation. Noteworthy, a change in the mean of the SST distribution increased black-browed albatross $\log(\lambda_s)$ despite increasing the frequency and magnitude of ECE (lower dots on figure 5). This pattern occurred because the historical SST mean was lower than the optimal value for the black-browed albatross, and there is a large plateau around the optimal value in the population response function. As a result larger environmental mean increased the occurrence of SST close to the optimal value that buffered the negative effect of ECE. The 'climate safety margin' (i.e. the difference between the optimal climatic conditions and the

historical climatic conditions) and the specific shape of the response function for a species may determine how ECE affects the stochastic population growth rate through a change in environmental mean. Single peak response functions like reported here are common [44], such as thermal performance curves in ectothermic species [46,47] (Fig. 5). A theoretical framework using such response functions [44] could shed light on the buffering role of the environmental mean against ECE as a function of the climate safety margins, the maximum height of the response function, the width of the range of optimal values, the rate of fall off from the optimal environment, as well as the asymmetry of the response function. Species with a large climate safety margin, a wide optimum range and a slow rate of fall off from the optimal environment, are likely less sensitive to ECE, especially when climate changes are dominated by a shift in the mean rather than a change in the standard deviation.

(c) Age dependent demographic responses to climate change

Individuals differ in their quality, age, sex and other characteristics that may mediate the effects of ECE on population growth and structure. For example, Welbergen *et al.* [48] showed higher susceptibilities of adult female Australian flying-foxes (*Pteropus alecto*) to temperature extremes, with potentially disproportionate effects on effective breeding population and recruitment. Here, we focused on the effect of age because like in humans [29], previous studies have found that older individual albatrosses were more likely die under warmer conditions than other age-classes in the population [33].

We found that for local changes, the population structure was altered by increases in both mean and standard deviation of SST, with opposed effects in middle-aged individuals, leading to a higher proportion of young individuals in the population. Old individuals were particularly affected by both changes in mean and standard deviation, suggesting a particular vulnerability to the frequency of ECE as reported in humans [29]. These changes were driven

by the age-specific non-linear relationships between vital rates and SST, more particularly by the decreasing survival of old individuals in both cold and warm SST ECE, the increasing breeding probability of young and middle aged individuals, and the increasing breeding success of young and old individuals when SST increased.

With future climate change, new concerns may arise for this black-browed albatross population because the structure of the population is projected to change with a higher proportion of juveniles, which are highly sensitive to other anthropogenic activities. Juveniles are known to represent a significant part of birds accidentally killed in long-line fisheries [36,38]. Rolland *et al.* (2009) demonstrated relationships between SST and fisheries impact on the growth rate of this same population. The stochastic population growth rate remains negative even when incorporating immigration in the young and middle-aged classes which is consistent with previous models and observations since 1976 [37]. This suggests that even at optimal values of SST, the population is likely affected by fisheries bycatch [37]. Mitigating the effect of fisheries with a warmer climate with limited change in environmental inter-annual variations may allow the population to recover. This will probably occur only for a short time as the climate safety margin (0.1°C) is relatively narrow compared to projected SST changes reported by the IPCC (≈1°C, [49]). A shift in mean SST by 1°C is not unlikely according to the IPCC projections. However, this would lead to a frequency of warm event of ~ 80%, and whether black-browed albatross will adapt to these conditions remains an open question. To predict the impact of extreme events and inform policy and management decisions, models linking IPCC climate projections to a demographic model would be required [23].

(d) Methodological considerations

The normal distribution is one possible distribution among many to address the relative impact in mean, variability as well as ECE. This distribution is symmetrical and thus does not account for the positive skewness that may result from climate change (i.e. more extreme warm than cold events [1]). To understand the effect of an increasing frequency of warm events, one could have used asymmetrical climate distributions, such as the generalized extreme value (GEV) distribution developed within the extreme value theory, which are designed to address the data sparseness problems in the tails of the distribution due to the rarity of extreme events.

[10,50]. In our case study, we could not apply such a distribution because our functional relationships between SST and vital rates were based on SST averaged over large temporal and spatial scales. Within extreme value theory GEV distributions are used to model the largest or smallest observations. For example, one can use the maximum SST recorded within a season or a spatial sector - the data are known as block maxima. For species such as ectotherms that are very sensitive to temperature daily minima or maxima, GEV distributions are very valuable [10]. However, long lived endothermic species, such as black-browed albatross, are likely to escape cold spells or heat waves because of their wide foraging range, their relatively good fasting abilities, or their ability to skip or abandon reproduction during extremely unfavourable events on the breeding grounds instead of jeopardizing their survival [13,51]. Thus, we believe that extreme environmental conditions for black-browed albatross more likely consist in persistent warmer SST over the entire breeding season and over a wide spatial sector, whereby their average value is extreme (i.e a compound ECE see [7]). As such, the normal is a useful approach when focusing on compound ECE defined over large spatial and temporal scales.

While previous studies have shed light on the respective role of the mean and standard deviation of the environment, few have focused on the shape of the distribution of the

environmental variables. Our framework was based on the normal distribution because it was the distribution that fitted the best our historical SST. It would have been interesting to apply the t-location-scale distribution that has heavier tails, meaning that it is more prone to producing ECE values, a property the normal distribution does not possess. This tail is influenced by the shape parameter of the t-location-scale distribution. In electronic supplementary material C, we applied such t-scale distribution to illustrate such approach, and over our historical range, the shape parameter was large, i.e. the t-location-scale distribution approaches the normal distribution. We show that the sensitivity of the black-browed albatross $\log(\lambda_s)$ with respect to the shape parameter of the t-location-scale distribution was almost null. This may appear counterintuitive given that the shape parameter affects the standard deviation of the distribution but, over our historical range, the shape parameter was large and, varied almost independently from the mean and the standard deviation of the distribution. Similarly to our study, [21,24] suggested that the effects of a change in the shape of the tail of the distribution set by the skew were generally small relative to those of environmental means or standard deviations.

Vasseur *et al*. [24] applied a transformation of an (initially) normally distributed temperature distribution to study the respective effects of the mean, standard deviation and positive skewness on the thermal performance of 38 ectothermic invertebrate species. They found that a change in the mean temperature distribution had a larger impact than a change in variability and skewness (their figure 2). The t-location-scale distribution could also be a useful framework when focusing on varying independently mean, standard deviation and shape of the environmental distribution, but would require changing the scale parameter in the t-location-scale distribution when varying the shape parameter, especially for lower values of the shape parameter (electronic supplementary material C).

To understand the role of ECE and changes in mean and standard deviation of SST on the demography of the black-browed albatross, we have projected the stochastic population growth rate and stable age structure using an age-structured population model [40]. These projections depend on age specific and climate dependent fecundity and mortality as well as assumptions on changes in climate variables. Models are very useful tools to understand the effect of climatic extremes that are rare, even if such projections require projecting beyond historical ranges of variability. Our study has indeed revealed contrasted patterns between values around the historical range and a wider range that depend on the climate safety margin. Although, we have projected the vital rates using functional relationships obtained with a robust capture-recapture analysis [33], to limit unrealistic demographic rates beyond the observed range, we have limited our wider range of climate parameters to few scenarios where we varied the two parameters of the SST distribution independently. Thus, we could not conduct a global sensitivity analysis that would require varying several model inputs simultaneously to account for interactions among parameters [52].

Finally, our approach focused on the effect of frequency and magnitude of extreme events on the long-term demography. But other ECE characteristics like the duration of a given ECE or a particular sequence of ECE (i.e. environmental auto-correlation) might also be important for the population [10]. Although the duration and sequence of ECE may affect greatly the transient population dynamics [53], they are likely to have little effect on the long-term population growth and structure for a long-lived species [4,54,55].

5. Conclusion

Our empirical study suggests how the direction and strength of change in population growth rate and population structure are determined by the mean and standard deviation of an environmental distribution, and shows that changes in the frequency and to a lesser extent the

magnitude of ECE, impact the demography of this black-browed albatross population. Interestingly, our results indicate that a shift in environmental mean can buffer and even reverse the effects of ECE on stochastic population growth rate. Species might therefore be able to cope with ECE. This depends on the magnitude of climate shift and variation in relation to a species' optimal environmental conditions.

Ethics. All experiments with albatrosses were approved by the Ethic Committee of the French Polar Institute (IPEV) and by the Comité de l'Environnement Polaire.

Authors' contributions. C.B. initiated the idea and H.W. supervised the long-term data necessary to this project. The study was conceived and designed by C.B., D.P. and S.J. The analyses were performed by D.P. and S.J. in consultation with C.B. and H.W. D.P., S.J. and C.B. wrote manuscript, and H.W. provided comments.

Competing interests. We have no competing interests.

Funding. Work carried out at Canyon des Sourcils Noirs was supported by Institut Paul Emile Victor (IPEV program n°109) and Terres Australes et Antarctiques Françaises. S.J. thanks support from NSF- Antarctic Sciences Division (project 1246407), the Grayce B. Kerr Fund and the Penzance Endowed Fund in Support of Assistant Scientists. D.P. PhD was supported by a grant from the French Research Minister CNRS-INEE.

Acknowledgements. We are extremely grateful to all field workers involved in the monitoring program of black-browed albatrosses at Kerguelen for 50 years. We thank Dominique Besson and Karine Delord for data management, Philippe Naveau, Hal Caswell, Lise Aubry, Dave Koon, Loreleï Guéry and Jean-Dominique Lebreton for fruitful discussions as well as D.P.'s PhD committee: Emmanuelle Cam, Daniel Oro, Jean-Michel Gaillard, Bernard Cazelles and Michael Schaub. We also thank Woods Hole Oceanographic

Institution's guest student program, Jamie Oliver from the British Antarctic Survey for help with the figures, Martjin Van de Pol and two anonymous reviewers for advice on how to improve this manuscript.

Figure 1. Sketch explaining the approach followed in this paper. Input environmental data consists of SST sampled into a normal distribution (middle-left). The observed SST from 1982 to 2015 was used to determine a threshold of warm ECE (top-left in red). We defined the ECE frequency as the occurrence of ECE, as well as the ECE magnitude as the maximum SST values occurring in the simulated environment. The population model projects the number of individuals within each age-class and is described by an age-structured life-cycle (middle-right) where vital rates depend on both age and SST (top-right). Vertical traits on the x-axis represent the occurrence of historical SST. The outputs are of two kinds (bottom): climatic, to measure the influence SST distribution parameters on the frequency and magnitude of warm SST ECE (1), and demographic, to measure the influence SST distribution parameters on the stochastic population growth rate and on the stable age distribution (2). It is also possible to combine the two outputs (3).

Figure 2. Sensitivity of the frequency and magnitude of warm SST ECE with respect to the two parameters of a normal distribution (mean and standard deviation) of sea surface temperature (SST). The distribution was fitted on 34 years of historical SST averaged in the foraging areas of Kerguelen black-browed albatrosses during the breeding season.

Figure 3. Sensitivity of the stochastic population growth rate $\log(\lambda_s)$ with respect to the two parameters of a normal SST distribution (mean and standard deviation).

Figure 4. Baseline stable age distribution (top) and sensitivity of the stable age distribution (bottom) with respect to the two parameters of a normal distribution (mean [μ] and standard deviation [σ]) of sea surface temperature (SST).

Figure 5. Stochastic population growth rate vary as a function of various SST distribution parameters over a wide range of variation. The mean of the normal SST distribution (plain line) could vary ± 1°C from the historical mean and the standard deviation of the normal SST distribution was multiplied by two (dots).

Figure 6. Relationships between the stochastic population growth rate $\log(\lambda_s)$ and frequency (top) and magnitude (bottom) of warm SST ECE according to changes of the two parameters of a normal distribution (mean [μ] increasing up to 1°C-grey circles and standard deviation [σ] multiplied by up to two-black squares). The size of markers increases proportionally to changes.

521 Figure 1

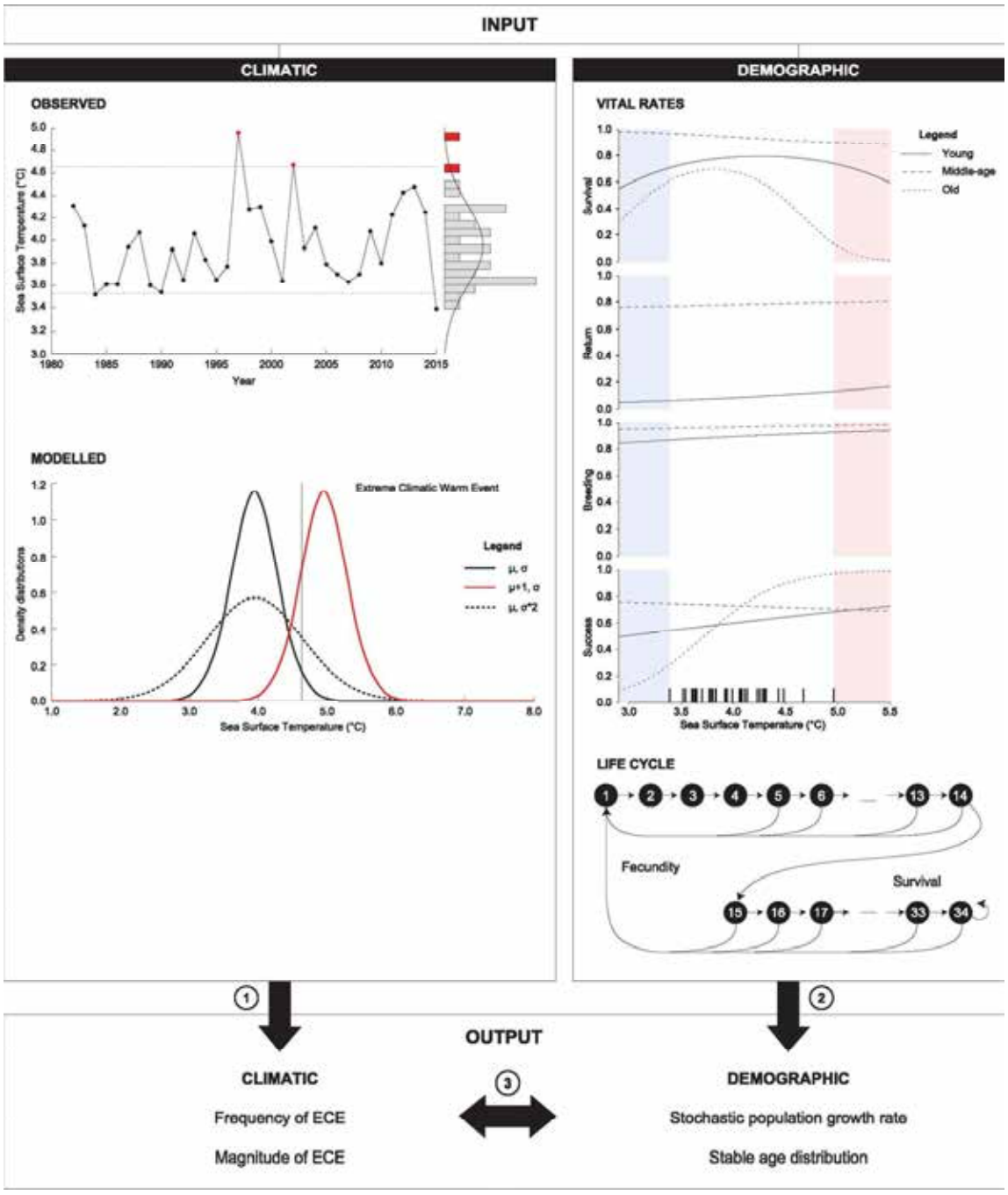

522

523 Figure 2

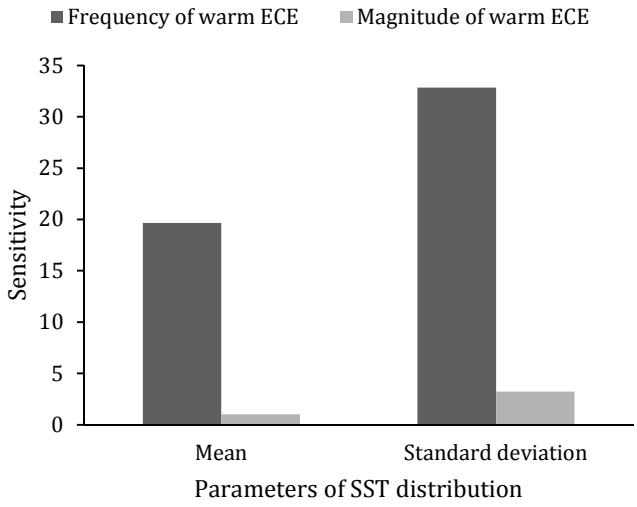

524

525

526

527 Figure 3

528

529

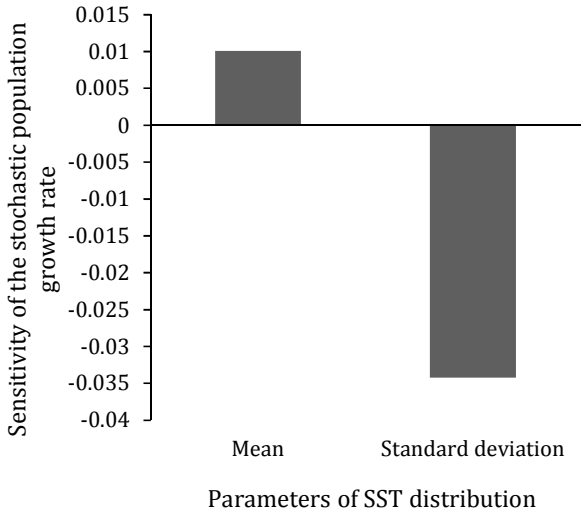

530

531

Figure 4

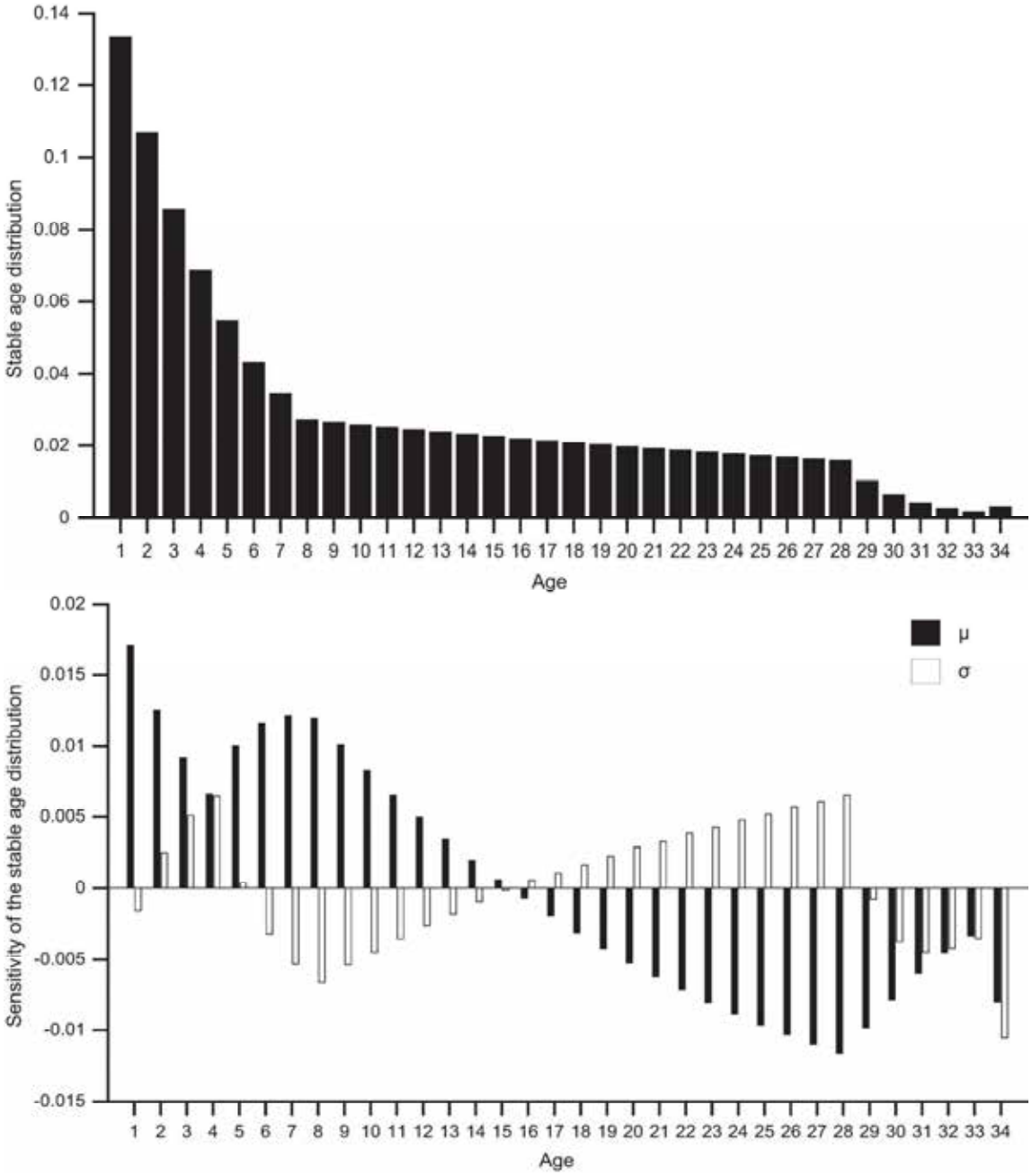
Stable age distribution
0.14
0.12
0.1
0.08
0.06
0.04
0.02
0
1 2 3 4 5 6 7 8 9 10 11 12 13 14 15 16 17 18 19 20 21 22 23 24 25 26 27 28 29 30 31 32 33 34
Age
Sensitivity of the stable age distribution
0.02
0.015
0.01
0.005
0
-0.005
-0.01
-0.015
μ
σ
1 2 3 4 5 6 7 8 9 10 11 12 13 14 15 16 17 18 19 20 21 22 23 24 25 26 27 28 29 30 31 32 33 34
Age

Figure 5

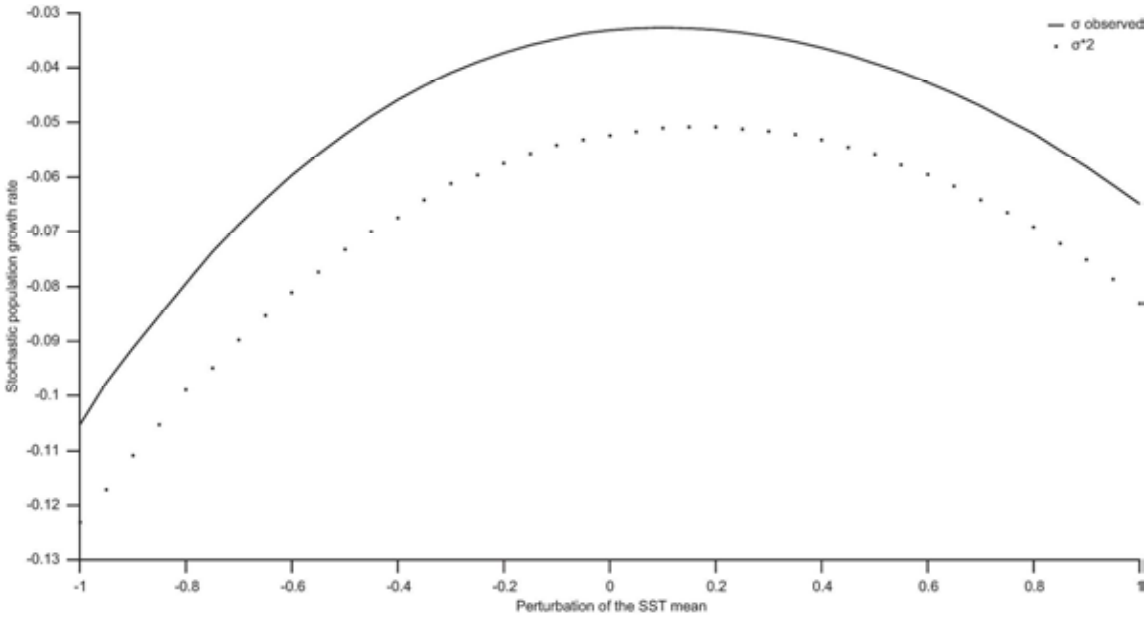
σ observed
σ^2
Stochastic population growth rate
-0.03
-0.04
-0.05
-0.06
-0.07
-0.08
-0.09
-0.1
-0.11
-0.12
-0.13
-1
-0.8
-0.6
-0.4
-0.2
0
0.2
0.4
0.6
0.8
Perturbation of the SST mean

Figure 6

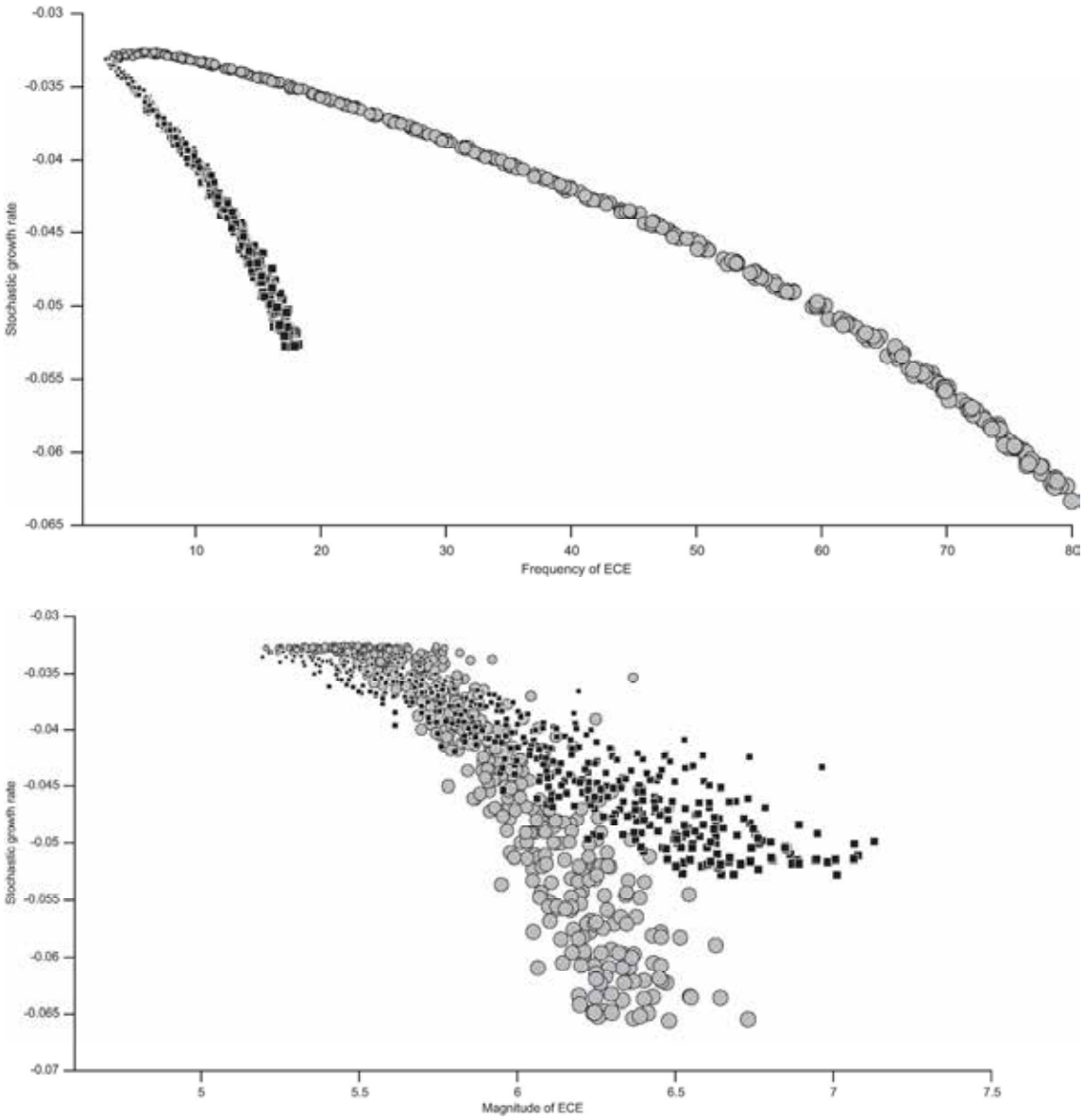
-0.03
-0.035
-0.04
-0.045
-0.05
-0.055
-0.06
-0.065
Stochastic growth rate
10
20
30
40
50
60
70
Frequency of ECE
-0.03
-0.035
-0.04
-0.045
-0.05
-0.055
-0.06
-0.065
-0.07
Stochastic growth rate
5
5.5
6
6.5
7
7.5
Magnitude of ECE

References

1. Managing the Risks of Extreme Events and Disasters to Advance Climate Change Adaptation. A Special Report of Working Groups I and II of the Intergovernmental Panel on Climate Change [Field, C.B., V. Barros, T.F. Stocker, D. Qin, D.J. Dokken, K.L. Ebi, M.D. Mastrandrea, K.J. Mach, G.-K. Plattner, S.K. Allen, M. Tignor, and P.M. Midgley (eds.)]. Cambridge University Press, Cambridge, UK, and New York, NY, USA, 582 pp.

2. Moreno, J. & Moller, A. P. 2011 Extreme climatic events in relation to global change and their impact on life histories. *Curr. Zool.* **57**, 375–389.

3. Stephenson, D. B., Casati, B., Ferro, C. a. T. & Wilson, C. A. 2008 The extreme dependency score: a non-vanishing measure for forecasts of rare events. *Meteorol. Appl.* **15**, 41–50. (doi:10.1002/met.53)

4. Palmer, G. et al. 2017 Climate change, climatic variation, and extreme biological responses. *PhilTransRSocLond B Biol Sci*

5. Felton, A. & Smith, M. 2017 Plant ecological responses to climate extremes from the organismal to the ecosystem level: an assessment of the role of scale. *PhilTransRSocLond B Biol Sci*

6. Altwegg, R., Visser, V., Bailey, L. & Erni, B. 2017 Learning from single extreme events. *PhilTransRSocLond B Biol Sci*

7. Van De Pol, M., Jenouvrier, S. & Visser, M. E. 2017 Ecological and evolutionary responses to extreme climatic events: challenges and research directions. *PhilTransRSocLond B Biol Sci*

8. Parmesan, C. et al. 1999 Poleward shifts in geographical ranges of butterfly species associated with regional warming. *Nature* **399**, 579–583.

9. Crick, H. Q. P., Dudley, C., Glue, D. E. & Thomson, D. L. 1997 UK birds are laying eggs earlier. *Nature* **388**, 526.

10. Kingsolver, J. G. & Buckley, L. B. 2017 Quantifying thermal extremes and biological variation to predict evolutionary responses to changing weather and climate. *PhilTransRSocLond B Biol Sci*

11. Bailey, L. D. & Pol, M. 2016 Tackling extremes: challenges for ecological and evolutionary research on extreme climatic events. *J. Anim. Ecol.* **85**, 85–96.

12. Jentsch, A., Kreyling, J. & Beierkuhnlein, C. 2007 A new generation of climate-change experiments: events, not trends. *Front. Ecol. Environ.* **5**, 365–374.

13. Jenouvrier, S., Péron, C. & Weimerskirch, H. 2015 Extreme climate events and individual heterogeneity shape life-history traits and population dynamics. *Ecol. Monogr.* **85**, 605–624. (doi:10.1890/14-1834.1)

14. Sanz-Aguilar, A., Daniel Anadon, J., Gimenez, A., Ballestar, R., Gracia, E. & Oro, D. 2011 Coexisting with fire: The case of the terrestrial tortoise Testudo graeca in

mediterranean shrublands. *Biol. Conserv.* **144**, 1040–1049. (doi:10.1016/j.biocon.2010.12.023)

15. Bull, J. J. & Vogt, R. C. 1979 Temperature-dependent sex determination in turtles. *Science* **206**, 1186–1188.

16. Glass, G. E. et al. 2000 Anticipating risk areas for hantavirus pulmonary syndrome with remotely sensed data: re-examination of the 1993 outbreak. *Emerg. Infect. Dis.* **6**, 238–247.

17. Thibault, K. M. & Brown, J. H. 2008 Impact of an extreme climatic event on community assembly. *Proc. Natl. Acad. Sci.* **105**, 3410.

18. Van De Pol, M. et al. 2010 Do changes in the frequency, magnitude and timing of extreme climatic events threaten the population viability of coastal birds? *J. Appl. Ecol.* **47**, 720–730.

19. Van De Pol, M., Vindenes, Y., Saether, B.-E., Engen, S., Ens, B. J., Oosterbeek, K. & Tinbergen, J. M. 2010 Effects of climate change and variability on population dynamics in a long-lived shorebird. *Ecology* **91**, 1192–1204.

20. Jenouvrier, S., Holland, M., Stroeve, J., Barbraud, C., Weimerskirch, H., Serreze, M. & Caswell, H. 2012 Effects of climate change on an emperor penguin population: analysis of coupled demographic and climate models. *Glob. Change Biol.*

21. Lawson, C. R., Vindenes, Y., Bailey, L. & van de Pol, M. 2015 Environmental variation and population responses to global change. *Ecol. Lett.* **18**, 724–736. (doi:10.1111/ele.12437)

22. Frederiksen, M., Daunt, F., Harris, M. P. & Wanless, S. 2008 The demographic impact of extreme events: stochastic weather drives survival and population dynamics in a long-lived seabird. *J. Anim. Ecol.* **77**, 1020–1029.

23. Jenouvrier, S. 2013 Impacts of climate change on avian populations. *Glob. Change Biol.* **19**, 2036–2057. (doi:10.1111/gcb.12195)

24. Vasseur, D. A., DeLong, J. P., Gilbert, B., Greig, H. S., Harley, C. D. G., McCann, K. S., Savage, V., Tunney, T. D. & O'Connor, M. I. 2014 Increased temperature variation poses a greater risk to species than climate warming. *Proc. R. Soc. Lond. B Biol. Sci.* **281**, 20132612. (doi:10.1098/rspb.2013.2612)

25. Chan, K. S., Mysterud, A., Øritsland, N. A., Severinsen, T. & Stenseth, N. C. 2005 Continuous and discrete extreme climatic events affecting the dynamics of a high-arctic reindeer population. *Oecologia* **145**, 556–563.

26. Jackson, S. T., Betancourt, J. L., Booth, R. K. & Gray, S. T. 2009 Ecology and the ratchet of events: climate variability, niche dimensions, and species distributions. *Proc. Natl. Acad. Sci.* **106**, 19685–19692.

27. Vindenes, Y., Edeline, E., Ohlberger, J., Langangen, Ø., Winfield, I. J., Stenseth, N. C., Vøllestad, L. A., Neubert, A. E. M. G. & Bronstein, E. J. L. 2014 Effects of Climate

641 Change on Trait-Based Dynamics of a Top Predator in Freshwater Ecosystems. *Am. Nat.*
642 **183**, 243–256. (doi:10.1086/674610)

643 28. Jenouvrier, S., Barbraud, C. & Weimerskirch, H. 2003 Effects of climate variability on
644 the temporal population dynamics of southern fulmars. *J. Anim. Ecol.* **72**, 576–587.

645 29. Stafoggia, M. et al. 2006 Vulnerability to heat-related mortality: a multicity, population-
646 based, case-crossover analysis. *Epidemiology* **17**, 315.

647 30. Pinaud, D. & Weimerskirch, H. 2002 Ultimate and proximate factors affecting the
648 breeding performance of a marine top-predator. *Oikos* **99**, 141–150.

649 31. Nevoux, M., Weimerskirch, H. & Barbraud, C. 2007 Environmental variation and
650 experience-related differences in the demography of the long-lived black-browed
651 albatross. *J. Anim. Ecol.* **76**, 159–167.

652 32. Rolland, V., Barbraud, C. & Weimerskirch, H. 2008 Combined effects of fisheries and
653 climate on a migratory long-lived marine predator. *J. Appl. Ecol.* **45**, 4–13.

654 33. Pardo, D., Barbraud, C., Authier, M. & Weimerskirch, H. 2013 Evidence for an age-
655 dependent influence of environmental variations on a long-lived seabird's life-history
656 traits. *Ecology* **94**, 208–220.

657 34. Weimerskirch, H. & Jouventin, P. 1998 Changes in population sizes and demographic
658 parameters of six albatross species breeding on the French sub-Antarctic islands. In
659 _*Albatross biology and conservation*_ (eds G. Robertson & R. Gales), pp. 84–91.
660 Chipping Norton, Australia: Surrey Beatty and Sons.

661 35. Cherel, Y., Weimerskirch, H. & Trouv,, C. 2000 Food and feeding ecology of the neritic-
662 slope forager black-browed albatross and its relationships with commercial fisheries in
663 Kerguelen waters. *Mar. Ecol. Prog. Ser.* **207**, 183–199.

664 36. Weimerskirch, H., Capdeville, D. & Duhamel, G. 2000 Factors affecting the number and
665 mortality of seabirds attending trawlers and long-liners in the Kerguelen area. *Polar Biol.*
666 **23**, 236–249.

667 37. Rolland, V., Nevoux, M., Barbraud, C. & Weimerskirch, H. 2009 Respective impact of
668 climate and fisheries on the growth of an albatross population. *Ecol. Appl.* **19**, 1336–1346.

669 38. Gales, R., Brothers, N. & Reid, T. 1998 Seabird mortality in the japanese tuna longline
670 fishery around Australia, 1988-1995. *Biol. Conserv.* **86**, 37–56.

671 39. Nevoux, M., Forcada, J., Barbraud, C., Croxall, J. & Weimerskirch, H. 2010 Bet-hedging
672 response to environmental variability, an intraspecific comparison. *Ecology* **91**, 2416–
673 2427.

674 40. Caswell, H. 2001 *Matrix population models: construction, analysis and interpretation*.

675 41. Nevoux, M., Weimerskirch, H. & Barbraud, C. 2010 Long- and short-term influence of
676 environment on recruitment in a species with highly delayed maturity. *Oecologia* **162**,
677 383–392.

42. Inchausti, P. & Weimerskirch, H. 2002 Dispersal and metapopulation dynamics of an oceanic seabird, the wandering albatross, and its consequences for its response to long-line fisheries. *J. Anim. Ecol.* **71**, 765–770.

43. In press. *MATLAB version 7.10.0. Natick, Massachusetts: The MathWorks Inc., 2010.*

44. García-Carreras, B. & Reuman, D. C. 2013 Are changes in the mean or variability of climate signals more important for long-term stochastic growth rate? *PloS One* **8**, e63974. (doi:10.1371/journal.pone.0063974)

45. Deutsch, C. A., Tewksbury, J. J., Huey, R. B., Sheldon, K. S., Ghalambor, C. K., Haak, D. C. & Martin, P. R. 2008 Impacts of climate warming on terrestrial ectotherms across latitude. *Proc. Natl. Acad. Sci.* **105**, 6668–6672.

46. Kingsolver, J. G., Diamond, S. E. & Buckley, L. B. 2013 Heat stress and the fitness consequences of climate change for terrestrial ectotherms. *Funct. Ecol.* **27**, 1415–1423.

47. Lloret, F., Escudero, A., Iriondo, J. M., Martínez-Vilalta, J. & Valladares, F. 2012 Extreme climatic events and vegetation: the role of stabilizing processes. *Glob. Change Biol.* **18**, 797–805.

48. Welbergen, J. A., Klose, S. M., Markus, N. & Eby, P. 2008 Climate change and the effects of temperature extremes on Australian flying-foxes. *Proc. R. Soc. Lond. B Biol. Sci.* **275**, 419–425.

49. Collins, M. et al. 2013 Long-term climate change: projections, commitments and irreversibility.

50. Coles, S. 2001 *An introduction to statistical modeling of extreme values*. Springer Verlag.

51. Barbraud, C., Delord, K. & Weimerskirch, H. 2015 Extreme ecological response of a seabird community to unprecedented sea ice cover. *R. Soc. Open Sci.* **2**, 140456. (doi:10.1098/rsos.140456)

52. Aiello-Lammens, M. E. & Akçakaya, H. R. 2016 Using global sensitivity analysis of demographic models for ecological impact assessment. *Conserv. Biol.*

53. Koons, D. N., Grand, J. B., Zinner, B. & Rockwell, R. F. 2005 Transient population dynamics: relations to life history and initial population state. *Ecol. Model.* **185**, 283–297.

54. Jenouvrier, S., Barbraud, C., Weimerskirch, H. & Caswell, H. 2009 Limitation of population recovery: a stochastic approach to the case of the emperor penguin. *Oikos* **118**, 1292–1298.

55. Ferguson, J. M., Carvalho, F., Murillo-García, O., Taper, M. L. & Ponciano, J. M. 2016 An updated perspective on the role of environmental autocorrelation in animal populations. *Theor. Ecol.* **9**, 129–148.

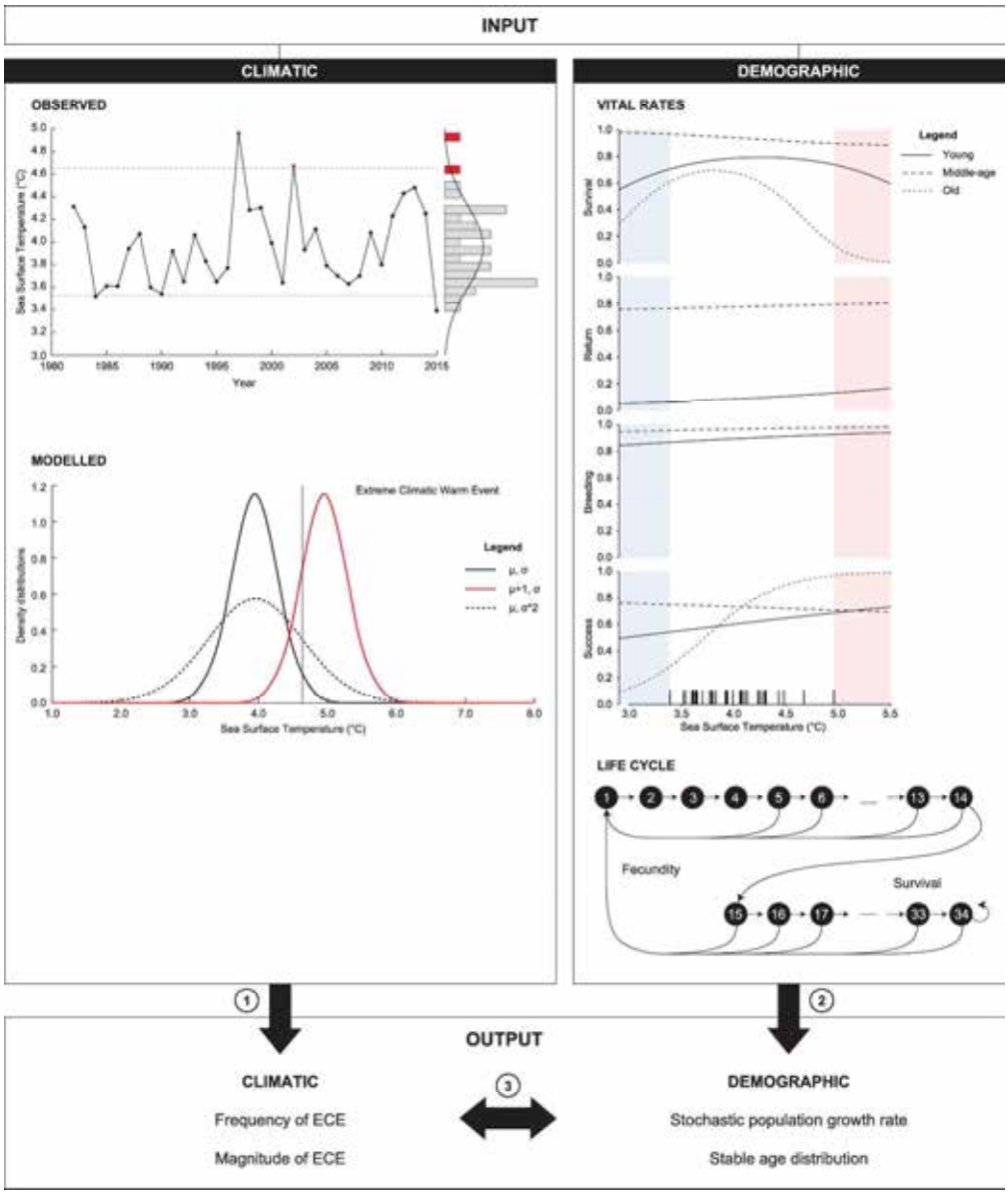

Sketch explaining the approach followed in this paper. Input environmental data consists of SST sampled into a normal distribution (middle-left). The observed SST from 1982 to 2015 was used to determine a threshold of warm ECE (top-left in red). We defined the ECE frequency as the occurrence of ECE, as well as the ECE magnitude as the maximum SST values occurring in the simulated environment. The population model projects the number of individuals within each age-class and is described by an age-structured life-cycle (middle-right) where vital rates depend on both age and SST (top-right). Vertical traits on the x-axis represent the occurrence of historical SST. The outputs are of two kinds (bottom): climatic, to measure the influence SST distribution parameters on the frequency and magnitude of warm SST ECE (1), and demographic, to measure the influence SST distribution parameters on the stochastic population growth rate and on the stable age distribution (2). It is also possible to combine the two outputs (3).

313x371mm (300 x 300 DPI)

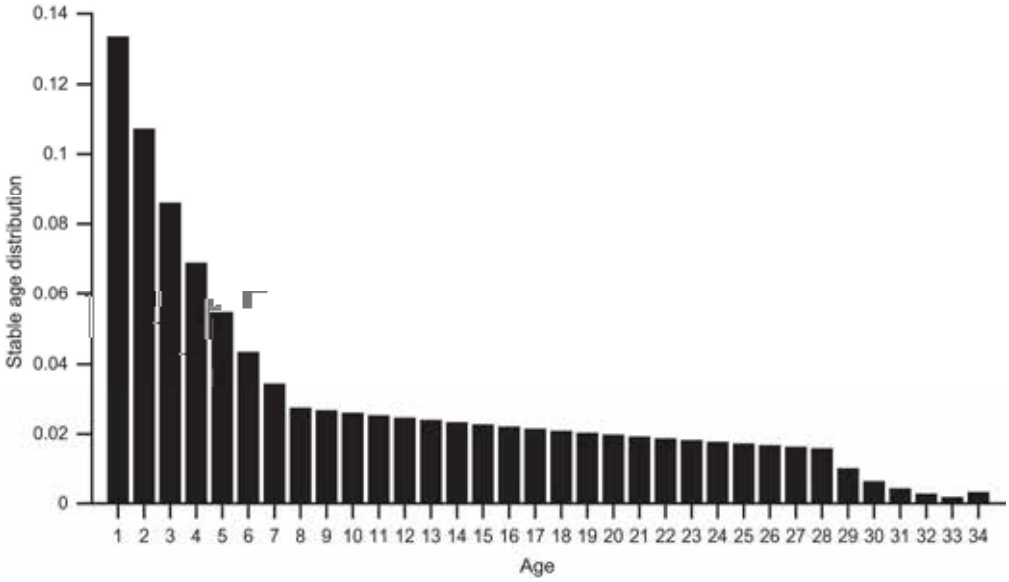

Baseline stable age distribution (top) and sensitivity of the stable age distribution (bottom) with respect to the two parameters of a normal distribution (mean [μ] and standard deviation [σ]) of sea surface temperature (SST).

248x143mm (300 x 300 DPI)

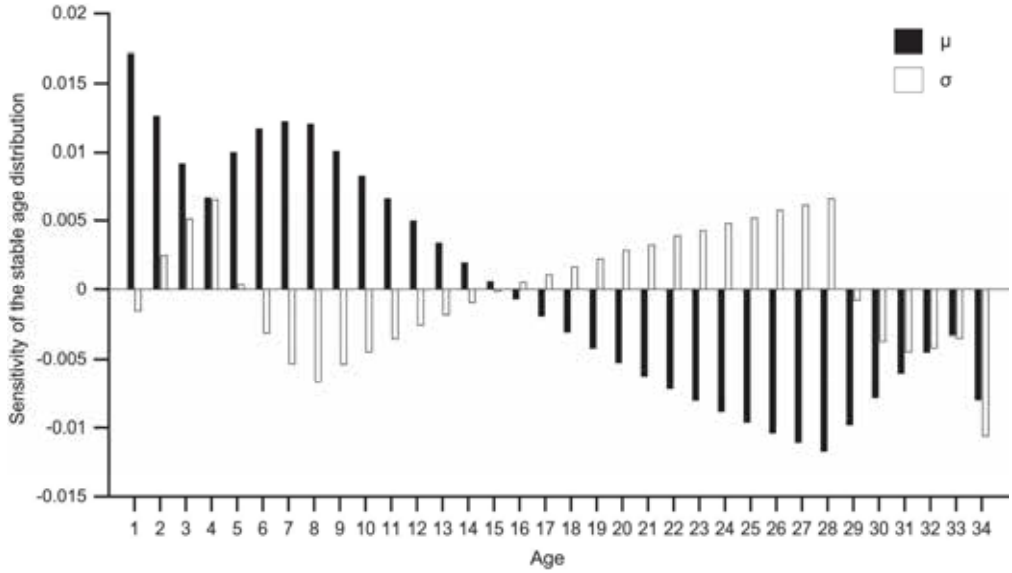

Baseline stable age distribution (top) and sensitivity of the stable age distribution (bottom) with respect to the two parameters of a normal distribution (mean [μ] and standard deviation [σ]) of sea surface temperature (SST).

248x141mm (300 x 300 DPI)

Stochastic population growth rate vary as a function of various SST distribution parameters over a wide range of variation. The mean of the normal SST distribution (plain line) could vary ± 1°C from the historical mean and the standard deviation of the normal SST distribution was multiplied by two (dots).

752x403mm (600 x 600 DPI)

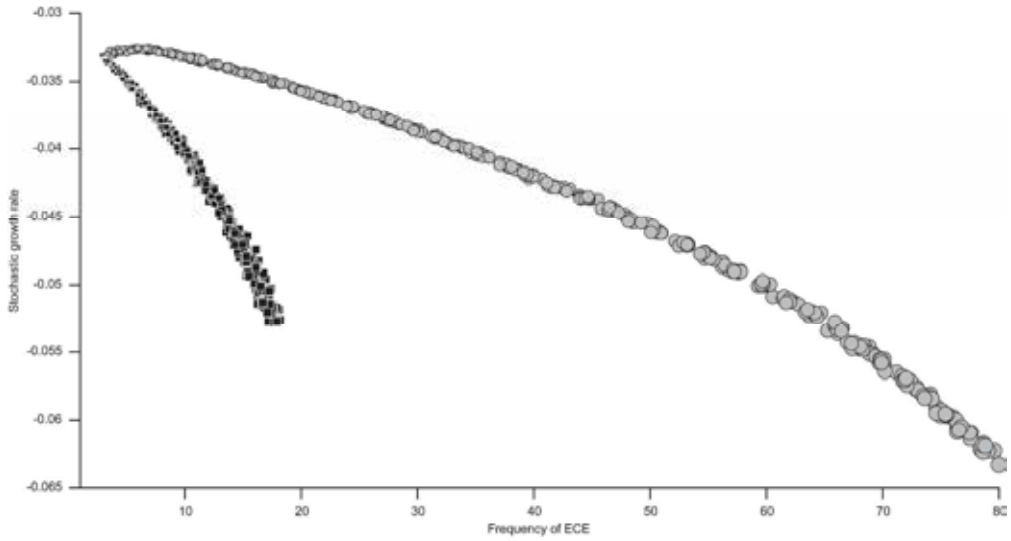

Relationships between the stochastic population growth rate log(λs) and frequency (top) and magnitude (bottom) of warm SST ECE according to changes of the two parameters of a normal distribution (mean [μ] increasing up to 1°C-grey circles and standard deviation [σ] multiplied by up to two-black squares). The size of markers increases proportionally to changes.

761x404mm (600 x 600 DPI)

Relationships between the stochastic population growth rate log(λs) and frequency (top) and magnitude (bottom) of warm SST ECE according to changes of the two parameters of a normal distribution (mean [μ] increasing up to 1°C-grey circles and standard deviation [σ] multiplied by up to two-black squares). The size of markers increases proportionally to changes.

821x387mm (600 x 600 DPI)